

NUMERICAL SIMULATION OF INFLUENCE OF THE NON-EQUILIBRIUM EXCITATION OF MOLECULES ON DIRECT DETONATION INITIATION BY SPARK DISCHARGE

*K.V. Korytcheko¹, A.N. Ozerov², D.V. Vinnikov², Yu.A. Skob³, D.P. Dubinin⁴,
R.G. Meleshchenko⁴*

¹*National Technical University “Kharkiv Polytechnic Institute”, Kharkov, Ukraine;*

²*National Science Center “Kharkov Institute of Physics and Technology”, Kharkov, Ukraine;*

³*National Aerospace University “Kharkov Aviation Institute”, Kharkov, Ukraine;*

⁴*National University of Civil Defence of Ukraine, Kharkov, Ukraine*

E-mail: korytchenko_kv@ukr.net

The influence of the non-equilibrium excitation of molecules on a direct detonation initiation by spark discharge was evaluated by a comparison of simulation result when the delayed vibrational excitation was taken into account with a result where the excitation effect was neglected. A numerical model of the spark channel expansion in chemically reacting gas was used. It was found out that increased critical energy of detonation initiation caused by the delayed activation of the vibrational excited states of polyatomic molecules in an initiating shock wave.

PACS: 52.80.Mg, 52.65.Yy

INTRODUCTION

Delayed activation of the vibrational excited states of polyatomic molecules affects the rates of chemical reactions behind the shock wave. Relaxation processes and its influence on the structure of shock and detonation waves have been investigated in [1 - 3]. Therefore, this process should be taken into consideration for the simulation of detonation initiation by the spark discharge.

The paper [4] describes the qualitative pattern of the distribution of thermodynamic parameters behind the detonation front as given in the Fig. 1. The kinetic energy of molecules is increased in the section 1-2. In the section 2-3 the rotational and vibrational energy of the molecules is increased due to the processes of translational-&-rotational relaxation and the translational-&-vibrational relaxation. In the section 3-5 that includes the induction zone (section 3-4) we observe the progress of chemical reactions.

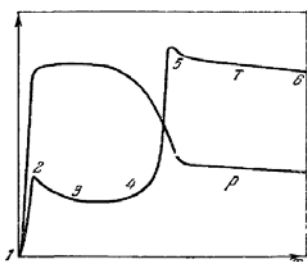


Fig. 1. The pressure and temperature distribution in the detonation wave according to [4]

Since the time of translational-vibrational relaxation can be commensurable with the induction period of chemical reactions, the nonequilibrium process of the molecule excitation can affect the parameters of the shock wave that provides the detonation initiation. With respect to the detonation initiation problem thermodynamic parameters become influential not only at the front of the generated shock wave but also behind the wave front as for their distribution. Therefore, this process must be taken into consideration for the model of direct initiation by the spark discharge.

The aim of present work is to study the influence of the non-equilibrium excitation of molecules on direct

detonation initiation by spark discharge. The influence was evaluated by a comparison of a simulation result when the delayed vibrational excitation was taken into account with a result where the excitation effect was “turn off”.

A NUMERICAL MODEL OF THE DIRECT DETONATION INITIATION BY SPARK DISCHARGE

The process of the detonation initiation by the spark discharge was described using the numerical model of spark channel expansion [5 - 7], supplemented by the source term in the energy equation that reflects the relaxation of the translational energy into the vibrational energy of the molecules and it was also supplemented by the differential equation of the conservation of vibrational energy of the modes with the source term. In this work the detonation initiation in the model was tested as applied to the stoichiometric hydrogen-oxygen mixture. A gas dynamic equation system (continuity, momentum and energy) was solved assuming one-dimensional radial problem statement for the multicomponent chemical-reactive gas mixture expressed as [8]

$$\frac{\partial \vec{a}}{\partial t} + \frac{1}{r} \frac{\partial (r\vec{b})}{\partial r} = \frac{1}{r} \vec{f}, \quad (1)$$

where vector columns are equal to:

$$\vec{a} = \begin{pmatrix} \rho \\ \rho u \\ \rho \varepsilon + \frac{\rho u^2}{2} \\ y_i \\ y_x e_x \end{pmatrix}, \quad \vec{b} = \begin{pmatrix} \rho u \\ p + \rho u^2 \\ u(\rho \varepsilon + \frac{\rho u^2}{2} + p) + k_r \frac{dT}{dr} \\ u y_i \\ u y_x e_x \end{pmatrix},$$

$$\vec{f} = \begin{pmatrix} 0 \\ p \\ r \cdot (\sigma E^2 - \sum_x \frac{de_x}{dt} - Q_{em}) \\ r \dot{\omega}_i \\ r \left[y_x \frac{de_x}{dt} + e_x \dot{\omega}_x \right] \end{pmatrix},$$

where ρ is the gas density; u is the velocity, p is the pressure, ε is the internal energy of gas per the mass unit of gas, k_T is the heat conduction coefficient, E is the electric field strength in the discharge channel column, σ is the plasma conductivity in the channel, W_{em} is the discharge energy radiation loss, r is the radial coordinate, t is the time, T is the translational temperature, y_i is the molar concentration of the i -th reactant, and ω_i is the chemical reaction rate of the i -th reactant (H_2O , H , O , OH , H_2O_2 , HO_2) of the mixture due to chemical reactions; $\dot{\omega}_x$ is the chemical reaction rate of the vibrational modes of molecular oxygen and hydrogen (H_2 , O_2); e_x is the vibrational energy of the vibrational modes; de_x/dt is the rates for vibration to translation/rotation energy transfer of the vibrational mode.

In the case of chemical reactions with the reactants of vibrational mode the reaction rate constant depends on the efficient temperature T_{ef} , expressed as

$$k_k(T_{ef,x}) = A_k \cdot T_{ef}^{n_k} \exp\left[-\frac{E_{ak}}{kT_{ef,x}}\right], \quad (2)$$

where $k_k(T_{ef,x})$ is the rate constant of the k -th reaction with the reactant of the vibrational mode depending on the efficient temperature T_{ef} ; A_k , n_k , E_{ak} are the coefficients in the generalized Arrhenius formula. In the reactions in which vibrational modes do not participate rate constants depend on translational temperature T .

The efficient temperature T_{ef} was expressed as [2]

$$T_{ef,x} = T^s T_{v,x}^{1-s}, \quad (3)$$

where s is the Park model parameter, $T_{v,x}$ is a temperature of the vibrational mode.

The computation of the current vibrational temperature $T_{v,x}$ of vibrational mode at a known current value of vibrational energy e_x was reduced to the derivation of the equation root from the following expression

$$e_x = U_x^0(T_{v,x}) - U_x^0(T_0) - C_{vx,T_0}(T_{v,x} - T_0), \quad (4)$$

where U_x^0 is the internal chemical and thermal energy of 1 mole of vibrational mode; C_{vx,T_0} is the molar heat capacity of vibrational mode; T_0 is the temperature at which the contribution of the vibrational heat capacity to the total heat capacity can be neglected (in the model $T_0 = 300$ K).

The model was tested by way of the comparison of the calculated parameters of the detonation wave with Chapman-Jouguet detonation wave parameters. The correctness of the function description that reflects the energy input from the external source was tested by the computation of available energy balance. The reliability of numerical model was previously confirmed by the satisfactory agreement of calculated and experimental data [5].

SIMULATION DATA OF DETONATION INITIATION BY SPARK DISCHARGE

The simulation data for the stoichiometric hydrogen and oxygen mixture where the excitation effect was neglected are given below. We assumed that $s = 1$ in this case. The initial mix temperature is assumed to be equal to $T = 300$ K, initial mixture pressure was equal to $p = 0.11$ MPa. The electric discharge circuit had the following parameters: the capacitor capacity was equal to

$C = 0.25$ μ F, the circuit inductance was equal to $L = 2$ μ H, active circuit resistance was equal to $R_C = 10$ m Ω . The initial voltage of capacity charge was equal to $U_{C0} = 10$ kV. The discharge gap length was $l_{sp} = 5$ mm.

The following distribution of thermodynamic parameters along the radial coordinate at different instants of time (Figs. 2-5) was obtained. Calculated distributions correspond to the following instants of time: 1 - $t_1 = 0.1$ μ s; 2 - $t_2 = 0.3$ μ s; 3 - $t_3 = 0.5$ μ s; 4 - $t_4 = 0.7$ μ s; 5 - $t_5 = 1$ μ s; 6 - $t_6 = 1.5$ μ s; 7 - $t_7 = 2$ μ s.

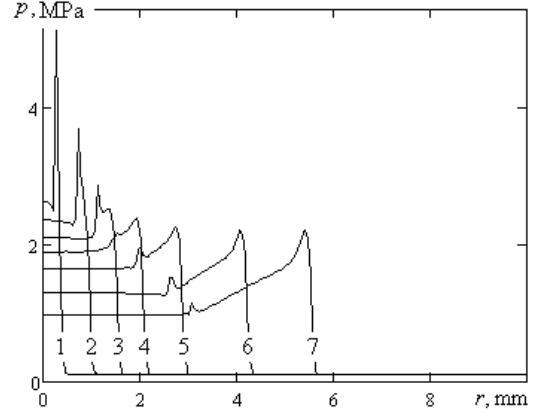


Fig. 2. Distribution of the pressure p along the radial coordinate r for the computation option [6]

Numerical computation data show that the computation option deals with the direct detonation initiation. The detonation wave velocity is $D = 2670 \pm 5$ m/s, the pressure jump at the detonation wave front reaches $p_f = 2.1 \pm 0.1$ MPa, the detonation product temperature is $T = 3500 \pm 100$ K, which satisfactorily agrees with detonation wave parameters for the given mixture. This proves the correctness of numerical algorithms used by the model to calculate the kinetics of chemical reactions, thermodynamic and gas dynamic processes.

The gas temperature in the current conducting channel reaches about 1 eV for the computation option, with respect to the order of magnitude it agrees with the data of other studies [9]. It should be noted that a higher temperature is reached at the initial stage of discharge progress, which also complies with experimental data.

During the detonation initiation by the spark discharge the current conducting channel functions as a permeable piston that pushes out the gas. The boundary permeability of current conducting channel specifies an increase in the gas mass in the given region.

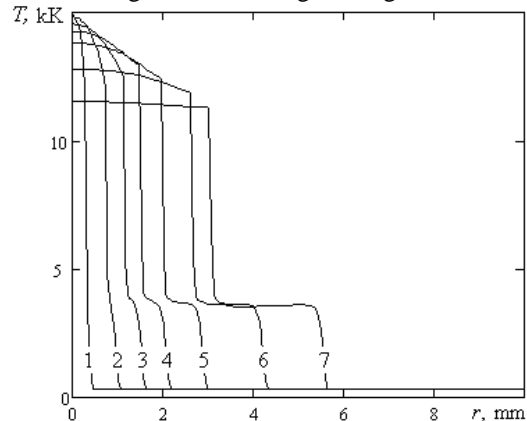


Fig. 3. Distribution of the Temperature T along the radial coordinate r for the computation option [6]

Therefore, during the expansion process of the current conducting channel of spark discharge energy expenditures for the dissociation process are increased.

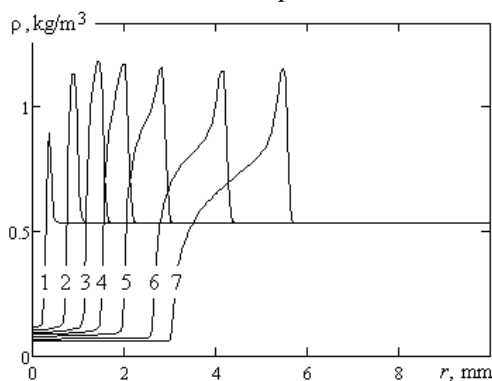


Fig. 4. Distribution of the gas mixture density ρ along the radial coordinate r for the computation option

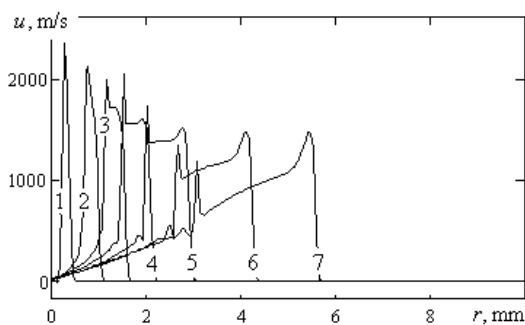


Fig. 5. Distribution of gas flow velocity u along the radial coordinate r for the computation option

At the initial stage of expansion the radius of current conducting channel actually coincides with that of shock wave front. Conditions for the hydrogen combustion, i.e. for the release of chemical energy arise in the region between the shock wave front and the current conducting channel. As the spark progress time is increased the area of the given region is enlarged. Assuming, a critical parameter that defines the initiation of self-sustained detonation is a minimum size of the region in which appropriate conditions for the combustion have been created. On termination of the additional supply of energy from the spark to the given region the propagation of self-sustained detonation in the combustion mixture must be provided. As the discharge time approaches the first half-period of discharge the current is reduced to low values and the input of energy into the spark from the discharge circuit is decelerated, accordingly and it is actually cut off. The propagation of self-sustained detonation approaching the first half-period of discharge is observed for the computation option.

The distribution of the molar density of components along the radial coordinate by the time $t = 2 \mu\text{s}$ is given in Fig. 6.

Fig. 6 shows that the density of atomic ions in the current conducting channel at the estimated time is one or two orders lower than the density of neutral atoms. The gas in the channel is strongly ionized. This is possible due to the fact that the cross-section of Coulomb collisions exceeds the cross-sections of other elastic collisions of electrons with the neutral plasma component by two or three orders of magnitude. The analysis data of distribution of the molar density of components

show the region in which the conditions for the hydrogen combustion were created.

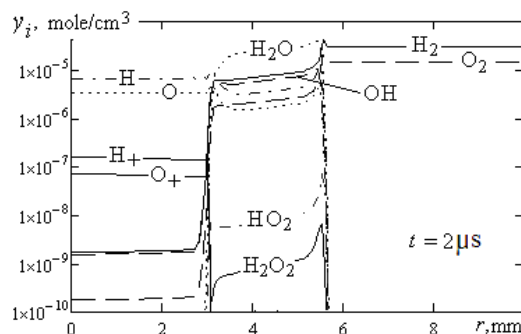


Fig. 6. Distribution of the molar density of components along the radial

The expansion of current conducting channel results in the dissociation of molecules including water molecules. This is one of the reasons for a low efficiency of the spark discharge in the detonation initiation problem, because actually the spark discharge energy provides the generation of shock wave that initiates the detonation. More efficient initiation would have been reached if the discharge current could provide not only the shock wave generation but also the gas heating due to the Joule heat before the wave front and after the wave front to reach the temperature at which combustion conditions are created.

The simulation data given above show that the detonation initiation in the stoichiometric hydrogen and oxygen mixture at normal initial conditions is reached at total expenditures of electric energy equal to 12.5 J. These data are at variance with experimental data obtained in the paper [10], where total energy expenditures for the detonation initiation surpassed this value by one order. It is assumed that this contradiction is related to the fact that the previous model of initiation takes into consideration no non-equilibrium excitation of molecules behind the shock wave front.

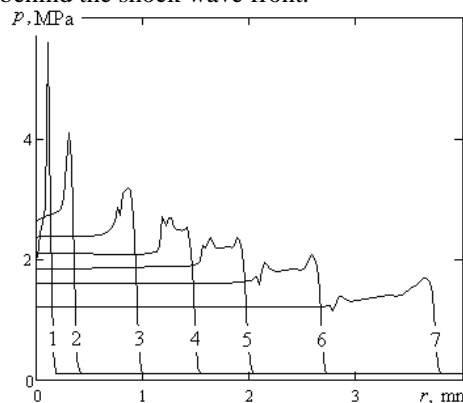


Fig. 7. Distribution of pressure p along the radial coordinate r for the computation option

To verify this assumption the simulation was carried out for the same initial parameters but taking into account the influence produced by the nonequilibrium excitation on the rate of chemical reactions. According to the research done in the paper [4], first the vibrational relaxation occurs behind the shock wave front, and then chemical reactions progress. On these grounds we assume that the vibrational temperature produces a key influence on the rate of chemical reactions. In this case

the parameter s in the Park model must take on a minimum value. For computations this parameter was assumed to be equal to $s = 0.1$.

The following distribution of thermodynamic parameters along the radial coordinate was obtained at different instants of time. Calculated distributions correspond to the following instants of time: $1 - t_1 = 0.03 \mu\text{s}$; $2 - t_2 = 0.1 \mu\text{s}$; $3 - t_3 = 0.3 \mu\text{s}$; $4 - t_4 = 0.5 \mu\text{s}$; $5 - t_5 = 0.7 \mu\text{s}$; $6 - t_6 = 1 \mu\text{s}$; $7 - t_7 = 1.5 \mu\text{s}$.

We come to the conclusion that the detonation initiation is not achieved at specified discharge conditions. This is proved by a drop in shock wave front pressure below the parameters of Chapman Jouquet wave, and by an increase in the separation of shock wave front from the flame wave front. A comparison of the distribution of the pressure, temperature and the molar density of components by the time $t = 1.5 \mu\text{s}$ shows that initially the gas mixture is heated behind the shock wave front (Fig. 7). The duration of the delay period depends on the shock wave intensity. Thus, for the computation option at the pressure jump of $p_{fr} = 2.5 \text{ MPa}$ at the shock wave front the length of the section related to the inflammation delay period is equal to about 0,2 mm. A decrease in the pressure at the shock wave front to $p_{fr} = 1.8 \text{ MPa}$ resulted in an increase of the length of this section up to 0.5 mm (Fig. 8).

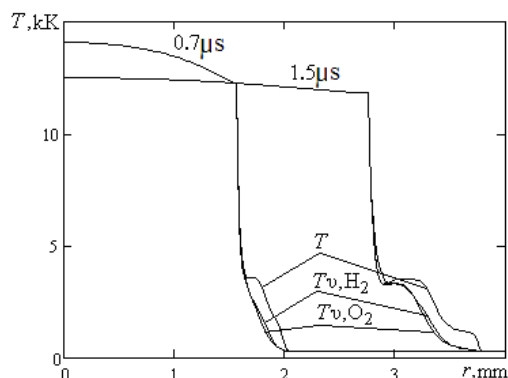


Fig. 8. Temperature distribution along the radial coordinate r for the computation option

The time of the vibrational relaxation of oxygen molecules exceeds to some extent the relaxation time of hydrogen molecules (Fig. 9). When the flame front reaches the vibrationally excited medium the relaxation rate is increased. This is caused both by a decrease in the number of vibrational modes due to the progress of chemical reactions and by the temperature rise of gaseous medium.

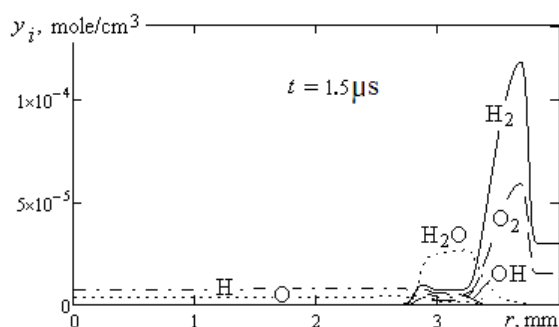


Fig. 9. Distribution of the molar density of components along the radial coordinate by the time $t = 1.5 \mu\text{s}$ for the computation option

The correctness of the assumption with regard to the value of parameter s is verified by the experimental investigation of the distance that is formed between the shock wave front and the flame front depending on the wave intensity.

This model was used for the investigation of detonation initiation at discharge circuit parameters that correspond to detonation initiation conditions in the experiment [10]. Therefore for the next computation option the electric discharge circuit had the following parameters: the capacitor capacitance was equal to $C = 2 \mu\text{F}$, the circuit inductance was equal to $L = 0.9 \mu\text{H}$, and the active circuit resistance was equal to $R_C = 10 \text{ m}\Omega$. The initial voltage of capacity charge was equal to $U_{C0} = 15 \text{ kV}$. The gas discharge gap length was $l_{sp} = 5 \text{ mm}$. For the Park model the parameter was assumed to be equal to $s = 0.1$.

The following distribution of thermodynamic parameters along the radial coordinate was obtained at different time instants (Figs. 10, 11). Calculated distributions correspond to the following instants of time: $1 - t_1 = 0.3 \mu\text{s}$; $2 - t_2 = 0.5 \mu\text{s}$; $3 - t_3 = 1 \mu\text{s}$; $4 - t_4 = 1.5 \mu\text{s}$; $5 - t_5 = 1.85 \mu\text{s}$; $6 - t_6 = 2.2 \mu\text{s}$.

In contrast to the previous computation option the detonation initiation takes place in this case. In other words the agreement with experimental data is available. The availability of detonation is reflected in that the combustion front is connected to the shock wave front, because the temperature jump occurs directly behind the wave front. Distribution of the molar concentration of components proves that the temperature jump is caused by the hydrogen combustion, because the concentration of water molecules is increased behind the wave front.

It should be noted that the required intensity of initiating shock wave is somewhat higher than in the model in which the vibrational nonequilibrium is not taken into account.

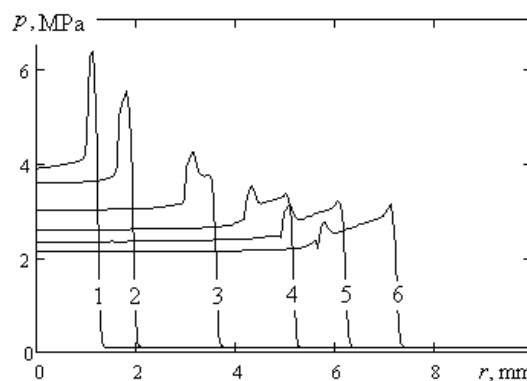


Fig. 10. Distribution of the pressure p along the radial coordinate r for the computation option

Thus, for computation conditions when the vibrational gas temperature separates from the translational gas temperature the pressure jump at the stationary shock wave front is equal to about $p_{fr} \approx 3 \text{ MPa}$ (Fig. 12), and in the conditions of equilibrium we have $p_{fr} \approx 2.3 \text{ MPa}$ (see Fig. 2). Such a difference can be explained by that the higher the intensity of shock wave the faster the progress of vibrational-translational relaxation is, and accordingly the combustion process behind the shock wave front is more intensive.

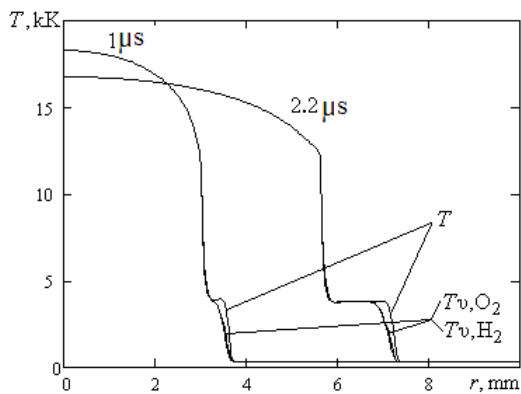


Fig. 11. Temperature distribution along the radial coordinate r for the computation option

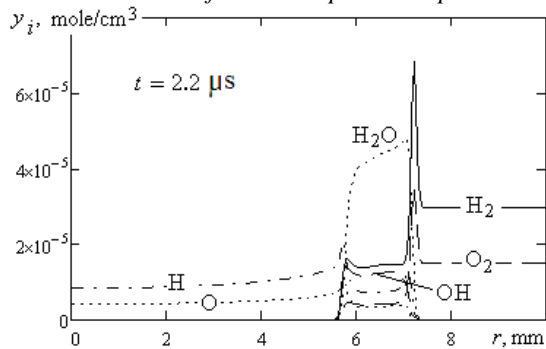


Fig. 12. Distribution of the molar density of components along the radial coordinate by the time $t = 2.2 \mu\text{s}$

Computations done to determine the propagation velocity of detonation wave using the estimation of the front advance of this wave show that it is equal to $D \approx 2860 \text{ m/s}$ for the computation option. This velocity value differs less from the experimental data in comparison with the designed velocity in the model that takes into account no nonequilibrium gas state. The temperature of detonation products was equal to about 3750 K.

The spark channel resistance is not linear (Fig. 13), therefore it is of interest to compare the quantity of energy released in the case of computation option with that calculated using the experimental data [10].

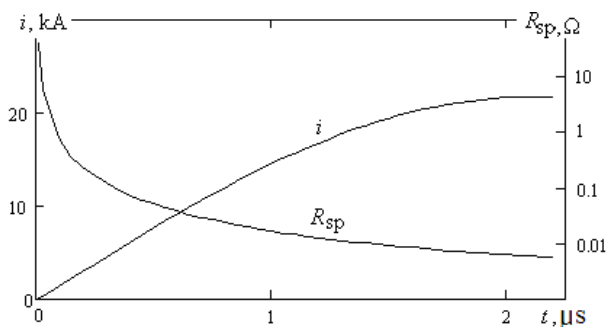


Fig. 13. A change in the discharge current i and the resistance R_x of the spark channel for the computation option

For the computation option the energy equal to about 6.5 J is released in the spark channel during $1/4$ of the discharge period (Fig. 14). According to the experimental data obtained by other researchers this value is equal to 10 J [10]. This difference is explained by the fact that the averaged resistance value of spark channel was used to process experimental data, which resulted in a substantial error during the data valuation. The pro-

cessing of experimental data also faces the difficulties related to the determination of the fraction of discharge energy lost in pre-electrode region. The premises give us every reason to assume the availability of satisfactory agreement between the experimental data and the calculated data.

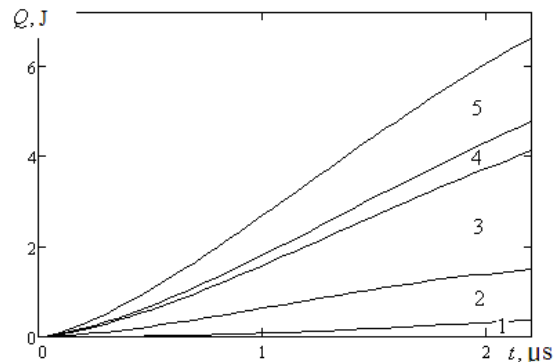


Fig. 14. Shared distribution in time of the discharge energy input into the spark:

- 1 – the radiation losses of discharge energy;
- 2 – the ionization energy; 3 – the dissociation energy,
- 4 – the kinetic energy of flow gas;
- 5 – the thermal energy

A shared distribution of input energy shows that a decrease in the efficiency of shock wave generated by the spark discharge is caused by a considerable absorption of discharge energy for the processes of ionization, dissociation and the radiation. A cumulative share of these expenditures by the time point of $t = 2.2 \mu\text{s}$ reaches 65%.

CONCLUSIONS

The obtained data speak in favor of the conclusion made in [11], according to which a considerable reduction in energy required for the detonation excitation is achieved due to the preliminary vibrational excitation of the molecules of combustible mixture. In this case it is sufficient to secure the vibrational temperature of about $T_0 \approx 2000 \text{ K}$ for the multiple reduction of critical initiation energy. In this case the data obtained using the model that takes into consideration no vibrational nonuniformity become correct. The corona discharge can be used for the vibrational medium excitation. Based on the analysis of simulation data it is recommended to perform the preliminary treatment of combustible gas mixture by the corona discharge prior to the high-current spark discharge to reduce the total expenditures of discharge energy for the detonation initiation.

REFERENCES

1. F. Mallinger. Numerical analysis of different vibrational relaxation models for master equations // *Institut national de recherche en informatique et en automatique*. 1997, September, Report 3263, 33 p.
2. V.Ju. Gidaspov, S.A. Losev, N.S. Severina. The nonequilibrium kinetics on the oxygen dissociation behind shock wave front // *Mathematical Models and Computer Simulations*. 2009, № 9(21), p. 3-15.
3. S. Ormode. Vibrational relaxation theories and measurements // *Rev. Modern Phys.* 1975, № 47, p. 193-258.

4. R.I. Solouhin. Detonation wave in gases // *Advance in physic science*. 1963, v. 80, № 4, p. 525-551.
5. K.V. Korytchenko, E.V. Poklonskiy, D.V. Vinnikov, D.V. Kudin. Numerical simulation of gas-dynamic stage of spark discharge in oxygen // *Problems of Atomic Science and Technology Series "Plasma Electronics and New Methods of Acceleration"*. 2013, № 4, p. 155-160.
6. K.V. Korytchenko, E.V. Poklonskii, P.N. Krivoshchev. Model of the spark discharge initiation of detonation in a mixture of hydrogen with oxygen // *Russ. J. Phys. Chem. B*. 2014, № 8, p. 692-700.
7. K.V. Korytchenko, V.I. Golota, D.V. Kudin, O.V. Sakun. Numerical simulation of the energy distribution into the spark at the direct detonation initiation // *Problems of Atomic Science and Technology. Series "Nuclear Physics Investigations"*. 2015, № 3, p. 154-158.
8. K.V. Korytchenko. High-voltage electric discharge technique for the generation of shock waves and heating the reacting gas. *Dr.Sc. Thesis National Technical University "Kharkov Polytechnic Institute"*. 2014.
9. Yu.P. Raiser. *Gas discharge physics*. M.: "Nauka", 1987, 592 p.
10. V. Kamenskihs, Ng. Hoi Dick, J.H.S. Lee. Measurement of critical energy for direct initiation of spherical detonations in stoichiometric high-pressure H₂-O₂ mixtures // *Combustion and Flame*. 2010, № 157, p. 1795-1799.
11. N.G. Dautov, A.M. Staric. Influence of vibrational excitation of molecules on combustion process in H₂+O₂ behind detonation shock wave // *Applied mechanics and technical physics*. 1955, № 36(6), p. 25-34.

Article received 01.06.2018

ЧИСЛЕННОЕ ИССЛЕДОВАНИЕ ВЛИЯНИЯ НЕРАВНОВЕСНОГО ВОЗБУЖДЕНИЯ МОЛЕКУЛ НА ПРЯМОЕ ИНИЦИИРОВАНИЕ ДЕТОНАЦИИ ИСКРОВЫМ РАЗРЯДОМ

К.В. Корытченко, А.Н. Озеров, Д.В. Винников, Ю.А. Скоб, Д.П. Дубинин, Р.Г. Мелещенко

Исследовано влияние неравновесного возбуждения молекул на прямое инициирование детонации искровым разрядом путем сравнения численных результатов моделирования в случае учета замедленного колебательного возбуждения с результатами расчетов без учета этого процесса. Для исследования использовалась математическая модель расширения искрового канала в реагирующем газе. Выявлено, что возрастание критической энергии инициирования детонации вызвано замедленным колебательным возбуждением многоатомных молекул в инициирующей ударной волне.

ЧИСЕЛЬНЕ ДОСЛІДЖЕННЯ ВПЛИВУ НЕРІВНОВАЖНОГО ЗБУДЖЕННЯ МОЛЕКУЛ НА ПРЯМЕ ІНІЦІЮВАННЯ ДЕТОНАЦІЇ ІСКРОВИМ РОЗРЯДОМ

К.В. Корытченко, О.М. Озеров, Д.В. Винников, Ю.А. Скоб, Д.П. Дубинин, Р.Г. Мелещенко

Досліджено вплив нерівноважного збудження молекул на пряме ініціювання детонації іскровим розрядом шляхом порівняння чисельних результатів моделювання у випадку урахування уповільненого коливального збудження з результатами розрахунків без урахування цього процесу. Для досліджень використано математичну модель розширення іскрового каналу в газі, що реагує. Виявлено, що зростання критичної енергії ініціювання детонації викликано уповільненим коливним збудженням багатоатомних молекул в ініціюючій ударній хвилі.